Hydrodynamics and Sedimentary Structures of Antidunes in Gravel and Sand Mixtures

P.A. Carling and R.M.D. Breakspear
School of Geography, Southampton, UK

S. Leclair
Environnement Illimitei Inc., Montreal, QC, Canada

ABSTRACT: Flume experiments using ADV and high-speed video show coherent and organized spatial pattern of turbulence above antidune bedforms. Initially, when antidune amplitude is small, turbulent stresses are equally distributed along the entire bed boundary layer, as antidune amplitude increases there is a progressive concentration of turbulent stresses in the near-bed region within the trough and on the upstream flank of the antidune immediately downstream. Antidunes break when turbulence reaches an 'intensity-threshold' above which rapid erosion occurs in the trough causing a pronounced increase in turbulent ejections laden with sediment and consequent rapid deposition on the downstream antidune flank. Flow then stalls over the downstream antidune, the standing wave collapses and erodes much of the bed. A clear distinction can be drawn between gravel and sand antidunes, with the former having turbulence stresses an order of magnitude higher than the latter. Two distinct types of antidune bedding were observed. Type I bedding is formed by widespread erosion and marks the lowest erosion surface during active antidune migration or collapse. Type II bedding is formed by turbulent sweeps during antidune growth and migration. Preservation is dependent on the amount of erosion of deposits during standing wave collapse.

1 INTRODUCTION

This study was undertaken in order to increase understanding of the hydrodynamics and sedimentary structures associated with antidunes which, compared with lower stage (ripples and dunes) and transitional (USPB) bedforms, have received relatively little attention. Antidunes are a relatively rare phenomena in the sedimentological record, because the sedimentary structures formed by antidunes are frequently destroyed by subsequent reworking. However preservation does occur in some environments, typically in highly aggrading situations, such as glacial outwash fans formed by jökulhlaups (Duller *et al*., in press). The identification of these bedforms, allows the inference of a high-energy environment with supercritical (shallow, fast) flow. Field geologists identify antidune deposits at outcrop and these inferences would be aided by detailed laboratory studies. Nelson *et al*. (1993) have stressed the need for an increased understanding of bedform process in order to inform palaeoenvironmental interpretation of exposures in the geological record.

2 METHOD

A small water-recirculating flume was used with working length of 6.5m, a width of 0.4m and a depth of 0.4m and pump capacity: 100 l/s. The slope can be adjusted up to 0.02 such that Froude numbers of between 0.1 and 2 are produced. A 25mm benthead Nortek ADV and an ECM were mounted on a movable instrument carriage at 0.5, 1, 2, 3, 4, 5, 6cm from bed down the central section of flow above 8 antidunes and data collected at 25Hz or 100Hz. Data was collected for 180 seconds at each location in the flow transects (giving at 100Hz, 18,000 measurements per record; and at 25Hz, 4,500 measurements per record); a record length that is compatible with the suggestions of Buffin-Bélanger and Roy (2005). Turbulence measurements were made a 3x4 array of experiments, either (1) sand skin roughness, (2) gravel skin roughness, or (3) porous gravel roughness with 4 different amplitudes to replicate growth of an antidune train (0.025m → 0.05m → 0.075m → 0.105m = incipient breaking). A high-speed PhotonFocus™ MV-D752 CMOS camera with a global shutter was used to obtain images of the flow.

Sedimentary structures were examined by sectioning sediments (Skipper *et al.*,1998) deposited by antidunes in a sand-gravel mixtures fed at the upstream evenly allowing a natural bed to aggrade, excess sediment being collected in a downstream sump.

3 RESULTS

3.1 *Turbulence*

The mean velocity, RMS, skew, TKE, Reynolds stresses, turbulence production and turbulence intensity fields were plotted for the 4 different amplitudes to replicate growth of an antidune train (0.025m → 0.05m → 0.075m → 0.105m = incipient breaking). In addition, the boundary layer correlation thickness, a measure of the thickness of the boundary layer was obtained and quadrant analysis conducted. An example of the flow field for TKE and Reynolds stress is shown in for 7.5cm amplitude gravel bedform wherein very high values of both parameters occur close to the bed in the trough between x = 30 and 40cm (Fig.1).

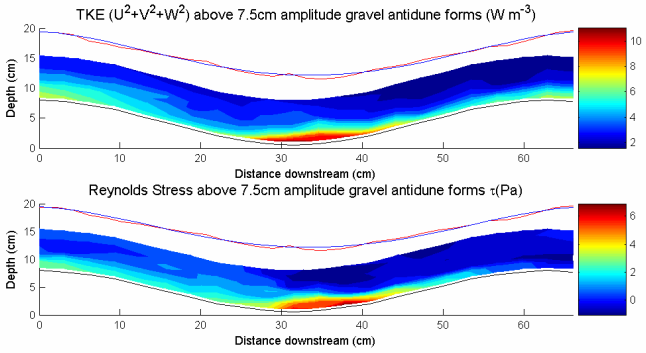

Figure 1: Turbulent kinetic energy and shear stress distributions over an antidune

Plots of TKE and Reynolds stresses (Fig.1) show close agreement, with stresses highest adjacent to the bed, especially on the upstream facing flank of the downstream antidune. An increase in TKE and Reynolds stress occurs with increasing amplitude, as well as the increasing concentration of stress in the trough region.

Quadrant analysis (not shown) shows that the for all quadrants, the most events above the hole size occur in the upper flow profile. Since previous studies, have concentrated on the bed to mid flow region, they have tended to not show this distribution, which in any case is of limited sedimentological importance due to its isolation from the bed. There are though significant sediment-entraining events adjacent to the bed occurring for between 0.5% and 3% of the velocity record. Investigation of the average $|u'v'|$ stresses during these events indicates that the highest $|u'v'|$ stresses occur adjacent to the bed. The distribution of stresses is initially relatively even, along the entire boundary layer, however for all quadrants it becomes increasingly concentrated in the trough region as antidune amplitude increases. In particular, $|u'v'|$ values during ejections increase from -0.08 in the boundary layer of 2.5cm amplitude antidunes, to -0.1 in the trough region of 5cm and 7.5cm amplitude antidunes. Likewise for sweeps, $|u'v'|$ values increase from -0.08 in the boundary layer of 2.5cm amplitude antidunes, to -0.095 in the trough region of 5cm and 7.5cm amplitude antidunes.

Plots of turbulence production, boundary layer correlation coefficient and turbulence intensity (not shown), support the above results and interpretations. Turbulence production is concentrated in the trough between each antidune bedform, maximum values, remaining at similar for 2.5, 5 and 7.5cm amplitude antidunes. The boundary layer correlation coefficient, a measure of the presence and integrity of any boundary layer, is relatively evenly distributed over 2.5cm antidunes, indicating a constant, developed boundary layer. However, with increasing antidune amplitude, it becomes increasingly disrupted, values becoming much higher in the trough region. McLean et al. (1994) found that low areas of correlation were associated with the dominance of the flow by outward interaction events – this fits well with data here, because lowest values occur as flow is moving up and away from the trough region (i.e. +ve u' and +ve v'). As for turbulence production, turbulence intensity is highest in the trough between each antidune for all three amplitudes of bedform. Values of turbulence intensity increase from 0.19, to 0.28 and the 0.5 with increasing antidune amplitude, indicating the increasingly turbulent hydrodynamic environment as antidunes steepen.

3.2 *Flow visualization*

Flow visualization and sequential time-lapse analysis of video still photographs were used to relate visually the bulk flow structure to the sediment response of the bed surface and the stratigraphy that was preserved following the passage of antidunes.

The images in Fig. 2 show the typical streaks produced by neutrally-buoyant pumice particles (frame rate: 50fps) over fixed gravel antidunes. Images are consecutive (i.e. with a 0.02 second gap between frames) from the downslope side of a bedform. Streaks throughout the flow profile are bed-parallel with limited temporal variation in trajectory. For the 2.5cm amplitude antidunes, streaks in the upper flow profile are again bed-parallel with limited temporal variations. However, in the lower flow profile, not all streaks are bed-parallel, with some streaks orientated at 30˚ upwards from bed-parallel. At the same location over 5cm and 7.5cm amplitude antidunes

(Fig. 2) variations in the lower flow profile are more notable. Generally streaks 'curve' over the trough region, but with some higher velocity trajectories entering the trough and penetrating to the bed.

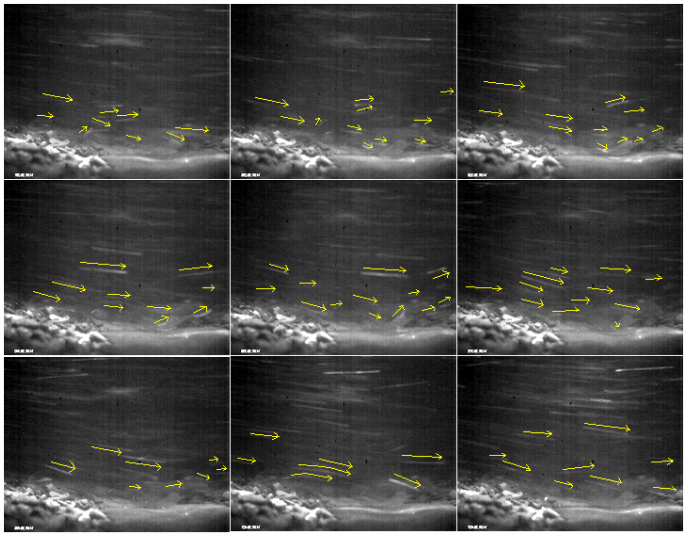

Figure 2 Temporal Distribution of Streaks over Medium (5cm) Amplitude Gravel Antidunes

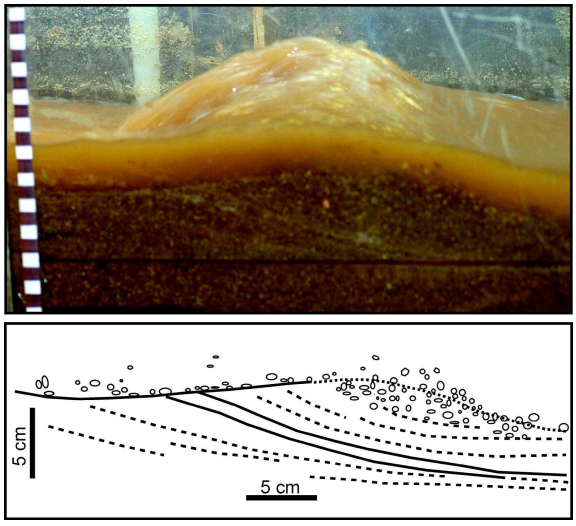

Figure 3 video still of flume experiment illustrating satnding wave over and antidune.

Figure 3 shows a video still, that relates the behaviour of a standing wave that is about to break with the sediment transport and stratigraphy developed within the associated antidune close to the flume wall. Series of such stills were used to describe the behaviour of growing and and breaking antidunes and the relationship through time to the bed stratigraphy.

3.3 *Sediment Transport and Stratigraphy*

Sediment transport was observed to occur by suspension, saltation and traction. These processes broadly corresponded to particle size, with the sand to granule element in suspension, granule to small gravel particles moving by saltation, and the gravel fraction moving as a 5mm – 15mm thick traction carpet. Within the traction carpet, individual grains could be discerned as moving by rolling and sliding. The traction carpet was observed to move with frequent thicker pulses (discrete low amplitude bedwaves of ~15mm amplitude (see Fig. 2)), these principally occurred leaving the trough region and moving up the flank of the next antidune. Sediment in the traction carpet, in particular sediment in the lower portion was seen to slow and stop on the upstream facing flank and crest of each antidune. Here, the majority of mobile grains within the traction carpet froze, with only grains near the bed surface continuing to move. Initially, occasional (every 10 to 5 seconds) sediment ejection events were observed. However as antidunes built these sediment ejection events became increasingly frequent (~1 second), carrying sediment from the trough onto the lower to mid portions of the downstream antidunes flank. The larger particles entrained typically followed a curved trajectory, landing approximately 100-150mm downstream. Coarse clasts could be seen accumulating at the crest, before being buried or periodically entrained downstream.

Figure 4 shows sets of deposits produced by antidune activity. The set produced by antidune activity is at the base, is between 50 and 100mm from the bed; and is c. 50mm thick. This set has a concave erosional base ('**eb**') and overlies undifferentiated sediment deposited at the beginning of the flume run. The top of the set of antidune deposits is gradational into the USPB set, which are plane bedded. The top section of the section is considered disturbed and is not evaluated here. The base of the set of antidune deposits is sand-rich relative to other sedimentology in the peel. Within the set, the cross-strata is defined by low-angle upstream-dipping concave-upwards backsets ('**ud**'), which onlap onto the erosional base of the set. Initially, backsets are sand-rich with lines of stringers – gravel clasts with their a-b axes parallel to the angle of dip. Later backsets are increasingly sand poor, with increasingly limited amounts of sand differentiating the backset deposits; the angle of gravel clasts a-b axes remains generally parallel to the angle of dip. Backsets are mostly concave upwards, and of varying thickness, from single clasts and 5mm of sand to several clasts thick (~ 5mm) and dip upstream at angles generally between 5.5˚ to 10.5˚ but up to 15˚ in places, with the base of backsets tending to dip at shallower angles. The main convex upwards outline above these convave upwards laminations represents the preserved remains of an antidune bedform. These backsets are truncated by a downstream-dipping erosional surface ('**ds**'), above which a concave-upward downstream-dipping wedge of coarser sediment ('**dd**') is present. The gradational transi-

tion between antidune sets to the USPB set above is characterized by undifferentiated sand-poor sediment ('**gt**'). The USPB set contains multiple, stacked planar laminae, alternating between sand-rich and sand-poor (marked '**sr**' and '**sp**' respectively).

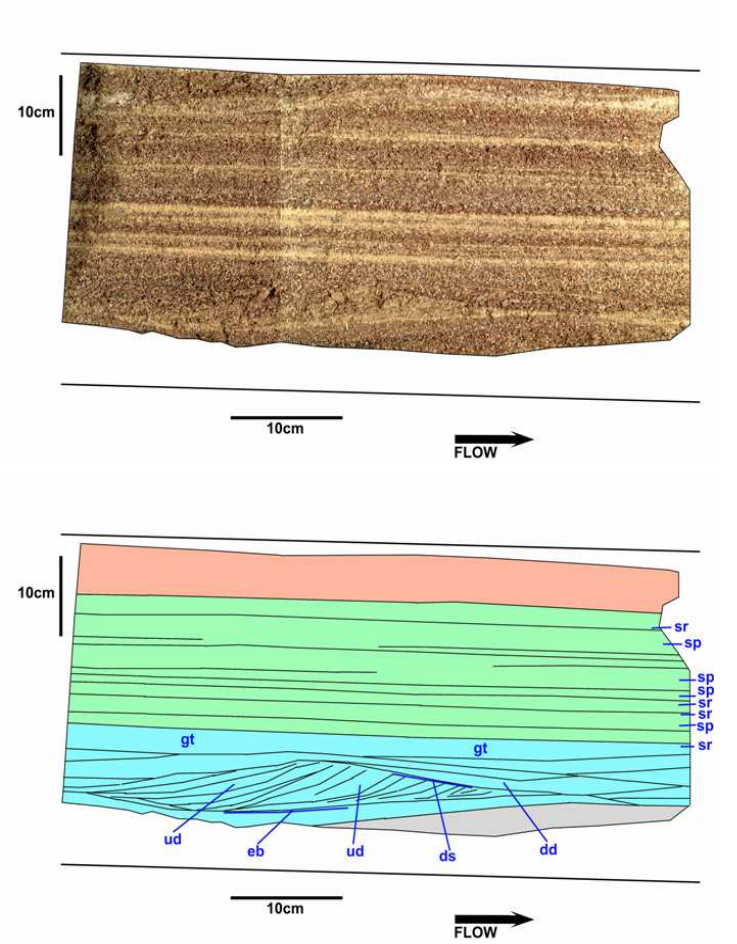

Figure 4 (top) image of deposits produced by antidune activity and (below) interpretation.

4 REFERENCES

Buffin-Bélanger, T. and Roy, A.G. (2005) 1 min in the life of a river: selecting the optimal record length for measurement of turbulence in fluvial boundary layers. *Geomorphology*, 68, 77-94.

Duller, R.A., Mountney, N.P., Russell, A.J. and Cassidy, N.C. (In Press) Architectural analysis of a volcanistic jökulhlaup deposit, southern Iceland: sedimentary Evidence for super-critical flow. *Sedimentology, on-line 8/02/08*

McLean, S.R., Nelson, J.M., Wolfe, S.R. (1994) Turbulence structure over two-dimensional bedforms: Implications for sediment transport. *Journal of Geophysical Research*, 99, 12729-12747.

Skipper, J.A., Ward, D.J. and Johnson, A. (1998) A rapid, lightweight sediment peel technique using polyurethane foam. *Journal of Sedimentary Research*, 68, 516–518